Research Article | Vol. 29, No. 7 / 29 March 2021 / Optics Express 10613
Optics EXPRESS

Layered antisymmetry-constructed clipped optical OFDM for low-complexity VLC systems

RUOWEN BAI AND STEVE HRANILOVIC*

Department of Electrical and Computer Engineering, McMaster University, ON, Canada
*hranilovic@mcmaster.ca

Abstract: In this paper, antisymmetry-constructed clipped optical orthogonal frequency division multiplexing (AC-OFDM) is proposed for visible light communication (VLC) systems, in which an antisymmetry property is imposed directly in time domain. AC-OFDM has nearly the same spectral efficiency and peak-to-average power ratio (PAPR) as traditional asymmetrically clipped optical OFDM (ACO-OFDM) but is less complex to implement. Layered AC-OFDM (LAC-OFDM) is then proposed as an extension to further improve spectral efficiency, where different layers of AC-OFDM signals are added in the time domain and transmitted simultaneously. Computational complexity analysis and numerical results show that LAC-OFDM has nearly the same spectral efficiency as layered asymmetrically clipped optical OFDM (LACO-OFDM) and enhanced unipolar OFDM (eU-OFDM) but is less complex. Specifically, LAC-OFDM requires less than half the multiplication and addition operations compared to the comparable LACO-OFDM scheme. Additionally, a pairwise iterative receiver for LAC-OFDM is proposed and its computational complexity is analysed. Monte Carlo simulation results show that LAC-OFDM requires nearly the same optical signal-to-noise ratio (OSNR) to achieve the same BER performance as LACO- and eU-OFDM.

1. Introduction

Visible light communications (VLC) adds a secondary communication channel to ubiquitous solid-state illumination devices [1–4] and is a candidate for future indoor broadband distribution. In VLC, data are modulated onto the instantaneous optical intensity emitted by a light-emitting diode (LED), i.e., intensity modulation (IM), and are detected by a photodiode (PD), i.e., direct detection (DD). As a result, all signals for VLC channels must be real, non-negative and have a bounded mean value [1–6].

The use of orthogonal frequency division multiplexing (OFDM) in VLC channels has been popular since illumination LEDs are typically low pass in nature. In order to make OFDM compatible with IM/DD VLC channels, direct current (DC) biased optical OFDM (DCO-OFDM) adds a DC bias to a conventional OFDM signal, consuming optical power while conveying no information [7]. To improve optical power efficiency, asymmetrically clipped optical OFDM (ACO-OFDM) [8], unipolar OFDM (U-OFDM) [9] and Flip-OFDM [10] were proposed, however, at a cost of half of the spectral efficiency. Enhanced U-OFDM (eU-OFDM) [9], layered ACO-OFDM (LACO-OFDM) [11], enhanced ACO-OFDM (eACO-OFDM) [12], spectral and energy efficient OFDM (SEE-OFDM) [13], and enhanced ACO-OFDM (EACO-OFDM) [14] were then proposed to retain the power efficiency of early approaches (i.e., no added DC bias) while improving spectral efficiency. LACO-OFDM and eU-OFDM work by combining different streams or layers of non-negative time-domain signals at the transmitter and successively detecting the modulated symbols at the receiver. The achievable information rate and optimal optical power allocation of LACO-OFDM are recently studied in [15–18], indicating that LACO-OFDM has a small gap to the capacity for the Gaussian optical intensity channels. Although eU- and LACO-OFDM have the advantages aforementioned, they suffer from high computational complexity to generate and demodulate streams or layers which may limit their application in simple and

#421108 https://doi.org/10.1364/OE.421108
Journal © 2021 Received 29 Jan 2021; revised 10 Mar 2021; accepted 10 Mar 2021; published 19 Mar 2021

Optics EXPRESS

energy efficient luminaires [19]. A low-complexity single-FFT receiver for LACO-OFDM was proposed and investigated in [20], which can reduce the computational complexity of the receiver. However, the reduction in complexity comes at the expense of approximately 2 dB power penalty at a bit error rate (BER) of 10^{-3} [20]. Reducing the complexity at both transmitter and receiver and retaining power efficiency remains a challenge for LACO-OFDM.

This paper proposes *antisymmetry-constructed clipped optical OFDM* (AC-OFDM) and layered AC-OFDM (LAC-OFDM) for VLC systems, extending our previous work in [21]. In AC-OFDM, an antisymmetric time domain signal is constructed, as in ACO-OFDM, however, all processing is done in time domain. Different from Flip-OFDM, which employs two OFDM frames to send portions of one OFDM symbol depending on their sign [10], AC-OFDM imposes anti-symmetry directly in time domain in a single OFDM frame. AC-OFDM employs a half-size inverse fast Fourier transform (IFFT) and a half-size fast Fourier transform (FFT) compared to ACO-OFDM and Flip-OFDM. Recently, and in parallel, an approach with a half-size FFT was proposed to reduce the complexity of only the receiver for hybrid asymmetrically clipped optical OFDM (HACO-OFDM) [22]. While [22] is similar in philosophy to our earlier work on AC-OFDM [21], in this work we present a general framework which applies at both the transmitter and the receiver as well as developing a layered modulation to improve spectral efficiency. LAC-OFDM sends information in different layers of AC-OFDM signals that are superimposed and detected successively. The spectral efficiency of LAC-OFDM is nearly two times bigger than ACO-OFDM, AC-OFDM and Flip-OFDM. Though LAC-OFDM is similar in philosophy to LACO-OFDM, it is shown to have a much simpler implementation which is more amenable to low cost, energy efficient, luminaires employed in VLC systems.

Compared to our previous conference paper [21], in this paper theoretical BER expressions for LAC-OFDM are derived to evaluate the reliability, which is aligned well with numerical results in the high signal-to-noise ratio (SNR) regime. The PAPR performance of LAC-OFDM is also evaluated and compared with its counterparts, which shows that the PAPR of LAC-OFDM is nearly the same as LACO-OFDM, and is smaller than that of eU-OFDM with the same number of layers/streams. Furthermore, a pairwise iterative receiver is proposed to further improve BER performance of AC-OFDM and LAC-OFDM. In the proposed pairwise iterative receiver, pairwise clipping is utilized in each AC-OFDM layer. This pairwise iterative receiver concept has also been extended to the case of eU-OFDM to improve BER performance. A computational complexity analysis is presented to compare this pairwise iterative receiver for LAC-OFDM to an improved receiver for LACO-OFDM [23] and to the pairwise iterative receiver for eU-OFDM. It is shown that LAC-OFDM is less complex for the same number of layers and the same number of iterations. Thus, for the same complexity, the pairwise iterative receiver for LAC-OFDM can employ more iterations and thus achieve greater BER gains compared to LACO-OFDM.

The balance of this paper is organized as follows. Section 2 introduces AC- and LAC-OFDM and makes connections to existing ACO-OFDM, eU-OFDM and LACO-OFDM techniques. The computational complexity and spectral efficiency of LAC-OFDM are analysed in Section 3 and a pairwise iterative receiver for LAC-OFDM is presented in Section 4. Numerical results of the computational complexity, BER, and PAPR performance are presented in Section 5. Finally, conclusions are drawn in Section 6.

2. System description

2.1. Background

In an ACO-OFDM system with N subcarriers, data symbols are only modulated onto the odd subcarriers, while the even subcarriers are set to zero [8]. Considering the Hermitian symmetry necessary to have a real-valued output, the input symbol vector to the inverse fast Fourier

Optics EXPRESS

transform (IFFT) is

$$\mathbf{X}_{\mathrm{ACO}} = \left[0, X_1, 0, X_3, 0, \ldots, 0, X_3^*, 0, X_1^*\right]^T \tag{1}$$

where $X_k, 1 \le k \le N-1$, is a complex symbol chosen from a quadrature amplitude modulation (QAM) constellation and $(\cdot)^T$ denotes the transpose operation. A consequence of using odd carriers only is that the output ACO-OFDM signal vector $\mathbf{x}$ of the IFFT is antisymmetric [8], i.e.,

$$x_n = -x_{n+N/2},\ 0 \le n \le N/2 - 1. \tag{2}$$

It has been shown that the non-negativity constraint can be satisfied by clipping the negative part of $\mathbf{x}$ directly with no distortion to the data being transmitted. The clipping distortion consists only of components at even subcarriers in the frequency domain and hence at the receiver side, symbols can be detected directly on the odd subcarriers [8].

Although, ACO-OFDM is optically power efficient, it has half of the spectral efficiency of traditional DCO-OFDM. To improve the spectral efficiency, LACO-OFDM was proposed where different layers of ACO-OFDM signals are summed in time domain and transmitted simultaneously [11]. In the l-th layer, LACO-OFDM modulates data onto subcarriers with index $2^{l-1}(2k+1), (k = 0, 1, \ldots, N/2^{l+1} - 1)$. Notice that for each layer, the sets of subcarriers used are disjoint. The output signal vector of the IFFT of each layer shares the antisymmetric property of ACO-OFDM and thus zero clipping is used to make the signal non-negative. The clipping distortion for a given layer distorts all higher layers and hence, the LACO-OFDM receiver demodulates lower layer ACO-OFDM symbols before higher layers.

2.2. *Antisymmetry-constructed clipped optical OFDM*

For an N-subcarrier AC-OFDM system, the transceiver block diagram is shown in Fig. 1.

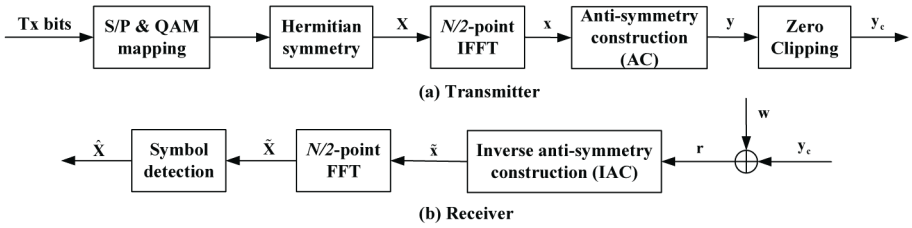

Fig. 1. Transceiver design block diagram for AC-OFDM.

At the transmitter, bits are mapped to QAM constellation symbols after serial-to-parallel (S/P) conversion. After Hermitian symmetry, the input symbol vector to the $N/2$-point IFFT is given by

$$\mathbf{X} = \left[0, X_1, X_2 \cdots, X_{N/4-1}, 0, X_{N/4-1}^*, \ldots, X_2^*, X_1^*\right]^T. \tag{3}$$

Notice that the AC-OFDM frame is of length $N/2$, rather than N for ACO-OFDM in (1), and that there is no requirement to use only odd subcarriers. The output of the $N/2$-point IFFT is given as

$$x_n = \frac{1}{\sqrt{N/2}} \sum_{k=0}^{N/2-1} X_k \exp\left(j\frac{2\pi}{N/2}nk\right),\ 0 \le n \le \frac{N}{2} - 1. \tag{4}$$

Prior to zero clipping, consider constructing the time-domain signal vector $\mathbf{y}$ using a process termed here as *antisymmetry construction* (AC) as

$$\mathbf{y} = [\mathbf{x}^T, -\mathbf{x}^T]^T. \tag{5}$$

Optics EXPRESS

Notice that $\mathbf{y}$ is antisymmetric, as in ACO-OFDM, i.e.,

$$y_n = -y_{n+N/2},\ 0 \le n \le N/2-1. \tag{6}$$

Similar to ACO-OFDM, the negative part of $\mathbf{y}$ can be clipped without any loss of information. Hence, applying zero clipping to $\mathbf{y}$ leads to the AC-OFDM signal

$$y_{c,n} = \frac{1}{2}(y_n + |y_n|),\ 0 \le n \le N-1 \tag{7}$$

where $|y_n|$ is the clipping distortion and $|\cdot|$ denotes the absolute value operation. Using (5) and (7), $\mathbf{y}_c$ can be written as

$$\mathbf{y}_c = \left[\frac{1}{2}\mathbf{x}^T + \frac{1}{2}|\mathbf{x}|^T, -\frac{1}{2}\mathbf{x}^T + \frac{1}{2}|\mathbf{x}|^T\right]^T. \tag{8}$$

Notice that $\mathbf{x}$ can be retrieved from $\mathbf{y}_c$ through the an *inverse antisymmetry construction* (IAC) operation

$$x_n = y_{c,n} - y_{c,n+N/2},\ 0 \le n \le N/2-1. \tag{9}$$

It is straightforward to show that the IAC operation proposed here also appears implicitly in the demodulation of traditional ACO-OFDM, however, it requires an N-point FFT. After a cyclic prefix (CP) is added to each OFDM symbol, a digital to analog converter (DAC) is employed. The resulting analog signal $y_c(t)$ is utilized to modulate an LED.

At the receiver, shot noise and thermal noise are well modelled as additive white Gaussian noise (AWGN) [2,8]. After sampling and discarding CP, the received signal is then given by

$$r_n = y_{c,n} + w_n,\ 0 \le n \le N-1 \tag{10}$$

where w_n is a sample of AWGN with standard deviation σ_w. Based on (9), an estimate of x_n can be obtained through the IAC operation as

$$\tilde{x}_n = r_n - r_{n+N/2}, 0 \le n \le N/2-1. \tag{11}$$

Define $\tilde{\mathbf{X}}$ as the $N/2$-point FFT of the received vector $\tilde{\mathbf{x}}$.

Finally, AC-OFDM can be detected symbol-by-symbol, i.e.,

$$\widehat{X}_k = \arg\min_{X\in\Omega_X} \left\| X - \widetilde{X}_k \right\|^2,\ k = 1, 2, \ldots, N/4-1 \tag{12}$$

where Ω_X denotes the constellation and $\|\cdot\|$ denotes the magnitude of a complex value.

Although a line-of-sight (LOS), flat VLC channel is assumed in this paper to aid in presenting the core idea and to compare with earlier work [8,9,12,13,16,20,23], AC-OFDM and later LAC-OFDM are applicable to dispersive channels. An equalization approach similar to those proposed for eU-OFDM [24] would be equivalently be applicable to AC- and LAC-OFDM.

2.3. Layered AC-OFDM

The transmitter block diagram for the proposed LAC-OFDM is shown in Fig. 2. Similar to traditional LACO-OFDM [11], different layers of AC-OFDM signals are added in the time domain and transmitted simultaneously to improve spectral efficiency.

In the l-th layer LAC-OFDM, an $N_{\mathrm{AC}}(l)$-point IFFT is utilized where

$$N_{\mathrm{AC}}(l) = \frac{N}{2^l}. \tag{13}$$

At each layer, AC-OFDM modulation is performed including an $N_{\mathrm{AC}}(l)$-point IFFT (4), antisymmetry construction (5) and zero clipping (7), resulting in the signal, $\mathbf{y}_c^{(l)}$, with length

Optics EXPRESS

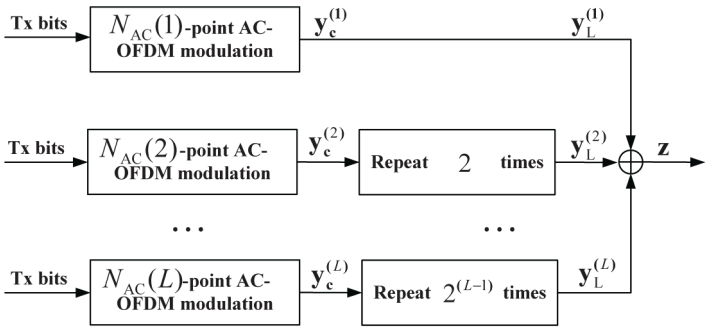

Fig. 2. Transmitter design block diagram for LAC-OFDM.

$2N_{AC}(l)$. Notice that, in contrast, a $2N_{AC}(l)$-point IFFT is used at layer l in the traditional LACO-OFDM. Similar to traditional LACO-OFDM [11], repeating $\mathbf{y}_c^{(l)}$ for 2^{l-1} times gives the l-th layer signal in LAC-OFDM

$$\mathbf{y}_L^{(l)} = [\underbrace{\mathbf{y}_c^{(l)^T}, \ldots, \mathbf{y}_c^{(l)^T}}_{\text{repeated } 2^{l-1} \text{ times}}]^T. \tag{14}$$

The LAC-OFDM signal vector, $\mathbf{z}$ is the summation of the L layers,

$$\mathbf{z} = \sum_{l=1}^{L} \alpha_l \mathbf{y}_L^{(l)} \tag{15}$$

where α_l is power allocation factor for each layer. To illustrate the core concepts, Fig. 3 presents an example of the waveforms at all layers for LAC-OFDM with $L = 3$ and $N = 64$. Though not explicitly shown in Fig. 2, this scaling is done to ensure that each layer has the same BER performance as discussed in Sec. 5.

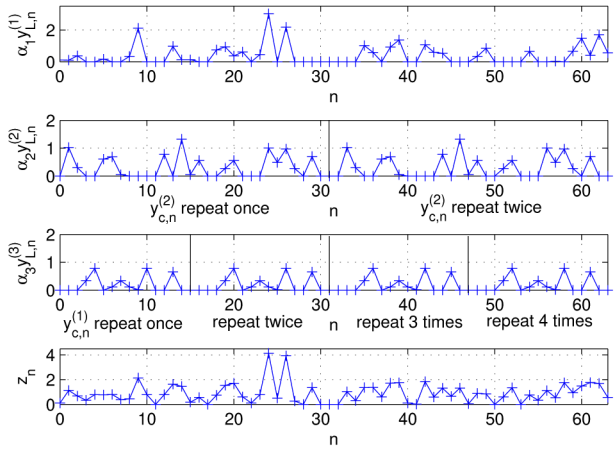

Fig. 3. An example of LAC-OFDM signal with $L = 3$ layers and $N = 64$ subcarriers (16 QAM is used and α_l defined in (48)).

At the receiver, LAC-OFDM is demodulated layer-by-layer in an analogous fashion to LACO-OFDM, as shown in Fig. 4. Since the clipping distortion of l-th layer only affects layers higher

Optics EXPRESS

than l, symbols in lower layers are detected first. Specifically, symbols $\widehat{\mathbf{X}}^{(1)}$ in the first layer are detected first through an $N/2$-point AC-OFDM demodulation including inverse antisymmetry construction (11), $N/2$-point FFT and symbol detection (12). Then the first layer AC-OFDM signal $\hat{\mathbf{y}}_L^{(1)}$ is reconstructed through $N/2$-point AC-OFDM modulation including $N/2$-point IFFT (4), antisymmetry construction (5) and zero clipping (7). The signal $\hat{\mathbf{y}}_L^{(1)}$ is subtracted from $\mathbf{r}$ leading to $\tilde{\mathbf{y}}_L^{(2)}$, which is used to demodulate the symbols $\widehat{\mathbf{X}}^{(2)}$ in the second layer.

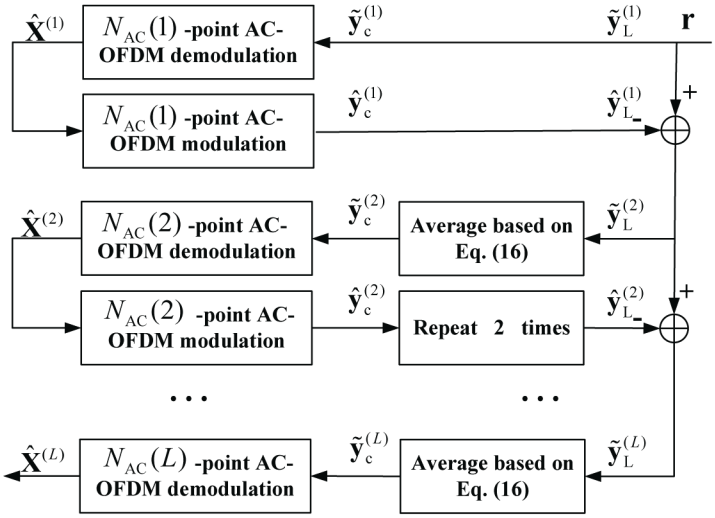

Fig. 4. Receiver design block diagram for LAC-OFDM.

For $l \geq 2$, as seen in Figs. 2 and 3, notice that $\mathbf{y}_c^{(l)}$ is repeated 2^{l-1} times in each frame. Taking advantage of this inherent repetition code in the frame of the LAC-OFDM signal, an estimate of the AC-OFDM signal $\tilde{\mathbf{y}}_c^{(l)}$ can be found by averaging over the repetitions in the frame as

$$\tilde{y}_{c,n}^{(l)} = \frac{1}{2^{l-1}} \sum_{q=0}^{2^{l-1}-1} \tilde{y}_{L,n+2qN_{\mathrm{AC}}(l)}^{(l)}, \quad 0 \leq n \leq 2N_{\mathrm{AC}}(l) - 1. \tag{16}$$

This repetition in the structure of the LAC-OFDM signal is also exploited in LACO-OFDM through the use of the N-point FFT operation. The remaining detection process is similar to the case for layer 1 described earlier with the signals reconstructed at each layer and subtracted from the received signal. To distinguish this receiver from the pairwise iterative receiver in Sec. IV.A, we denote this receiver as *simple receiver* for LAC.

It is interesting to note that this receiver structure combines the layered approach of LACO-OFDM [11] with the time-domain processing of the receiver from eU-OFDM [9].

3. Complexity analysis

3.1. Computational complexity assumptions

In this section, the computational complexity of LAC-OFDM is quantified by counting the number of real-valued multiplication and addition operations required and comparing them to the requirements for LACO- and eU-OFDM.

According to [25], for an N-point IFFT or FFT module using Cooley-Tukey decomposition and N a power of 2, $M(N)$ real-valued multiplication operations (RMOs) and $A(N)$ real-valued

Optics EXPRESS

addition operations (RAOs) are required where

$$M(N) = 2N\log_2(N) - 4N + 4 \tag{17}$$

and

$$A(N) = 3N\log_2(N) - 2N + 2. \tag{18}$$

In the subsequent analyses, our underlying assumption is that operations such as clipping or antisymmetry construction (5) do not require any arithmetic operations as they can be efficiently implemented via switching logic. Additionally, the complexity of detecting individual symbols on carriers is not included in this analysis and will be the same for all schemes considered.

3.2. Computational complexity: transmitter

At the LAC-OFDM transmitter, each layer requires an FFT of length $\frac{N}{2^l}$. Hence, the number of required RMOs and RAOs for an N-subcarrier LAC-OFDM system with L layers are

$$M^{(t)}_{\text{LAC}}(L,N) = \sum_{l=1}^{L} M\left(\frac{N}{2^l}\right) = \left(1 - \frac{1}{2^L}\right)2N\log_2(N) - \left(8 - \frac{L+4}{2^{L-1}}\right)N + 4L \tag{19}$$

and

$$A^{(t)}_{\text{LAC}}(L,N) = \sum_{l=1}^{L} A\left(\frac{N}{2^l}\right) + (L-1)N = \left(1 - \frac{1}{2^L}\right)3N\log_2(N) - \left(9 - L - \frac{3L+8}{2^L}\right)N + 2L. \tag{20}$$

Using a similar analysis, for traditional LACO-OFDM with N subcarriers and L layers, the RMOs and AMOs are [18]

$$M^{(t)}_{\text{LACO}}(L,N) = \sum_{l=1}^{L} M\left(\frac{N}{2^{l-1}}\right) = \left(1 - \frac{1}{2^L}\right)4N\log_2(N) - \left(12 - \frac{2L+6}{2^{L-1}}\right)N + 4L \tag{21}$$

and

$$A^{(t)}_{\text{LACO}}(L,N) = \sum_{l=1}^{L} A\left(\frac{N}{2^{l-1}}\right) + (L-1)N = \left(1 - \frac{1}{2^L}\right)6N\log_2(N) - \left(11 - L - \frac{3L+5}{2^{L-1}}\right)N + 2L. \tag{22}$$

For eU-OFDM with N subcarriers and L streams, the RMOs and RAOs averaged over an OFDM super frame are [18]

$$M^{(t)}_{\text{eU}}(L,N) = \frac{1}{2^L}\sum_{l=1}^{L} 2^{L-l}M(N) = \left(1 - \frac{1}{2^L}\right)\left(2N\log_2(N) - 4N + 4\right) \tag{23}$$

and

$$A^{(t)}_{\text{eU}}(L,N) = \frac{1}{2^L}\left(\sum_{l=1}^{L} 2^{L-l}A(N) + (L-1)2^L N\right) = \left(1 - \frac{1}{2^L}\right)\left(3N\log_2(N) - 2N + 2\right) + (L-1)N. \tag{24}$$

Comparing the dominant terms of $M^{(t)}_{\text{LAC}}(L,N)$ and $A^{(t)}_{\text{LAC}}(L,N)$ to $M^{(t)}_{\text{LACO}}(L,N)$ and $A^{(t)}_{\text{LACO}}(L,N)$, LAC-OFDM requires only half the RMOs and half the RAOs as traditional LACO-OFDM. Though the complexity of LAC-OFDM and the averaged complexity eU-OFDM are comparable, LAC-OFDM has the advantage of lower latency since the transmitting signal is N-samples long while eU-OFDM transmits a signal of length $2^L N$-samples. Numerical comparisons of complexity are presented in Sec. 5.

Optics EXPRESS

3.3. Computational complexity: receiver

To detect the l-th layer of the AC-OFDM signal ($1 \le l \le L-1$), an $N_{\mathrm{AC}}(l)$ point FFT is required followed by an $N_{\mathrm{AC}}(l)$ point IFFT. For the last layer, i.e., $l = L$, only an $N_{\mathrm{AC}}(L)$ point FFT is required since signal reconstruction is not necessary. Thus, LAC-OFDM requires $M^{(r)}_{\mathrm{LAC}}(L,N)$ RMOs where

$$M^{(r)}_{\mathrm{LAC}}(L,N) = 2\sum_{l=1}^{L-1} M\left(\frac{N}{2^l}\right) + M\left(\frac{N}{2^L}\right) = \left(1-\frac{3}{2^{L+1}}\right)4N\log_2(N) - \left(16-\frac{3L+10}{2^{L-1}}\right)N + 8L - 4. \tag{25}$$

Similarly, the number of RAOs can be computed, however, three additional steps are required. Averaging of the received samples is done in each layer following (16) to take advantage of the structure of each layer followed by the IAC operation, defined in (9). Also, the interference of lower layers must be removed from higher layers. The resulting number of real additions required is

$$\begin{aligned} A^{(r)}_{\mathrm{LAC}}(L,N) &= 2\sum_{l=1}^{L-1} A\left(\frac{N}{2^l}\right) + A\left(\frac{N}{2^L}\right) + \underbrace{\sum_{l=1}^{L}\left(1-\frac{1}{2^{l-1}}\right)N}_{\text{Averaging (16)}} + \underbrace{\sum_{l=1}^{L}\frac{N}{2^l}}_{\text{IAC (9)}} + \underbrace{N(L-1)}_{\text{Subtraction of lower layers}} \\ &= \left(1-\frac{3}{2^{L+1}}\right)6N\log_2(N) - \left(18-2L-\frac{9L+19}{2^L}\right)N \quad + 4L - 2. \end{aligned} \tag{26}$$

For LACO-OFDM with receiver proposed in [11], in which inter-layer interference (ILI) is removed in frequency domain, the total number of real arithmetic operations are

$$M^{(r)}_{\mathrm{LACO}}(L,N) = 2\sum_{l=1}^{L-1} M\left(\frac{N}{2^{l-1}}\right) + M(N) = \left(1-\frac{\frac{8}{5}}{2^L}\right)10N\log_2(N) - \left(28-\frac{L+2}{2^{L-4}}\right)N + 8L - 4 \tag{27}$$

and

$$A^{(r)}_{\mathrm{LACO}}(L,N) = 2\sum_{l=1}^{L-1} A\left(\frac{N}{2^{l-1}}\right) + A(N) + \sum_{l=1}^{L-1}\frac{N}{2^l} = \left(1-\frac{\frac{8}{5}}{2^L}\right)15N\log_2(N) - \left(21-\frac{12L+7}{2^{L-1}}\right)N + 4L - 2. \tag{28}$$

As shown in [18], the complexity of LACO-OFDM receiver can be reduced by removing ILI from the lower layers in the time domain before demodulating each layer. The required RMOs and RAOs in this case are

$$M^{(r)}_{\mathrm{LA}}(L,N) = \left(1-\frac{3}{2^{L+1}}\right)8N\log_2(N) - \left(24-\frac{6L+14}{2^{L-1}}\right)N + 8L - 4 \tag{29}$$

and

$$A^{(r)}_{\mathrm{LA}}(L,N) = \left(1-\frac{3}{2^{L+1}}\right)12N\log_2(N) - \left(23-2L-\frac{9L+10}{2^{L-1}}\right)N + 4L - 2. \tag{30}$$

For the same N and L, $M^{(r)}_{\mathrm{LA}}(L,N)$ and $A^{(r)}_{\mathrm{LA}}(L,N)$ are smaller than $M^{(r)}_{\mathrm{LACO}}(L,N)$ and $A^{(r)}_{\mathrm{LACO}}(L,N)$, respectively, since an N-point FFT is used once in the receiver to remove ILI in the time domain while it is used twice in the receiver with removing ILI in the frequency domain.

Optics EXPRESS

For eU-OFDM, the RMOs and RAOs averaged over an OFDM super frame are [18]

$$M_{\mathrm{eU}}^{(r)}(L,N)=\frac{1}{2^L}\left(2\sum_{l=1}^{L-1}2^{L-l}M(N)+M(N)\right)=\left(1-\frac{3}{2^{L+1}}\right)\left(4N\log_2(N)-8N+8\right) \tag{31}$$

and

$$\begin{aligned}A_{\mathrm{eU}}^{(r)}(L,N)&=\frac{1}{2^L}\left(2\sum_{l=1}^{L-1}2^{L-l}A(N)+A(N)+\sum_{l=1}^{L}\left(2^{l-1}-1\right)\frac{2^LN}{2^{l-1}}+\sum_{l=1}^{L}2^{L-l}N+2^L(L-1)N\right)\\&=\left(1-\frac{3}{2^{L+1}}\right)6N\log_2(N)-\left(6-2L-\frac{7}{2^L}\right)N+4-\frac{6}{2^L}.\end{aligned} \tag{32}$$

Observing the dominant terms of $M_{\mathrm{LAC}}^{(r)}(L,N)$ and $A_{\mathrm{LAC}}^{(r)}(L,N)$ with $M_{\mathrm{LACO}}^{(r)}(L,N)$ and $A_{\mathrm{LACO}}^{(r)}(L,N)$, the proposed receiver for LAC-OFDM requires less than half complexity than the traditional LACO-OFDM. As is the case with the transmitter, the receiver of LAC-OFDM requires nearly the same complexity as eU-OFDM on average. However, LAC-OFDM also has an advantage of lower latency at the receiver since each symbol can be decoded from N received samples while eU-OFDM requires 2^LN received samples for demodulation [9].

3.4. Spectral efficiency analysis

In LAC-OFDM, L layers of AC-OFDM signals are added together in the time domain and transmitted simultaneously. The spectral efficiency can be calculated by

$$\Upsilon_{\mathrm{LAC}}^{(L)}=\frac{\sum_{l=1}^{L}\left(\frac{N}{2^{l+1}}-1\right)\log_2 M_l}{N+N_{\mathrm{CP}}} \tag{33}$$

where M_l is constellation size of QAM utilized in l-th layer and N_{CP} is assumed to be length of CP. If the constellation size for each layer is set to be the same, $M_l=M$, (33) can be rewritten as

$$\Upsilon_{\mathrm{LAC}}^{(L)}=\frac{1}{2}\left(1-\frac{1}{2^L}\right)\frac{N}{N+N_{\mathrm{CP}}}\log_2(M)-\frac{L}{N+N_{\mathrm{CP}}}\log_2(M). \tag{34}$$

For LACO-OFDM, the spectral efficiency is given by [11]

$$\Upsilon_{\mathrm{LACO}}^{(L)}=\frac{1}{2}\left(1-\frac{1}{2^L}\right)\frac{N}{N+N_{\mathrm{CP}}}\log_2(M) \tag{35}$$

while for eU-OFDM with N subcarriers and L streams, spectral efficiency is [9]

$$\Upsilon_{\mathrm{eU}}^{(L)}=\frac{1}{2}\left(1-\frac{1}{2^L}\right)\frac{N-2}{N+N_{\mathrm{CP}}}\log_2(M). \tag{36}$$

For LACO-OFDM and LAC-OFDM, the number of layers L cannot be greater than $\log_2 N-1$. For a given N and $L\le\log_2 N-1$, LACO-OFDM has the largest spectral efficiency while LAC-OFDM has the smallest spectral efficiency. However, in the case when N is large

$$\lim_{N\longrightarrow\infty}\frac{L}{N}\log_2(M)=0 \tag{37}$$

and $\Upsilon_{\mathrm{LAC}}\rightarrow\Upsilon_{\mathrm{LACO}}$. Hence, for large N

$$\Upsilon_{\mathrm{LAC}}^{(L)}\approx\Upsilon_{\mathrm{eU}}^{(L)}\approx\Upsilon_{\mathrm{LACO}}^{(L)}=\frac{1}{2}\left(1-\frac{1}{2^L}\right)\frac{N}{N+N_{\mathrm{CP}}}\log_2(M). \tag{38}$$

Spectral efficiency comparisons between LAC-OFDM and its counterparts for different constellation sizes is shown in Fig. 5, where $N=1024$. It can be seen that the spectral efficiency of LAC-OFDM is nearly the same as eU- and LACO-OFDM when the same constellation size and the same number of layers/streams are employed.

Optics EXPRESS

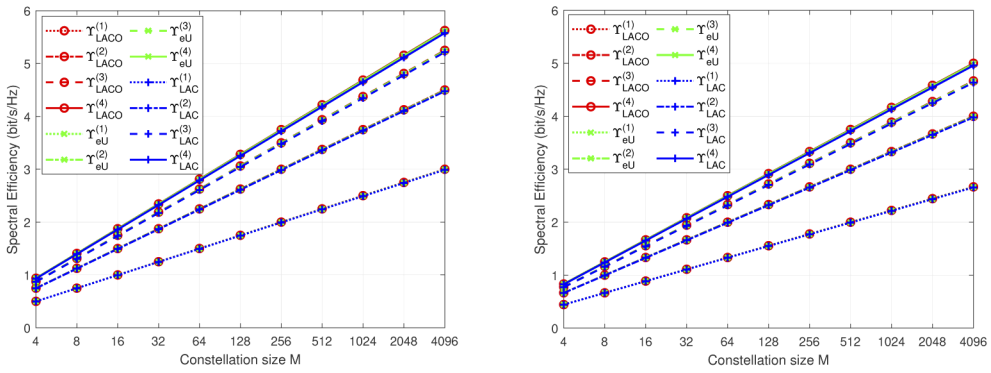

(a) $N_{\mathrm{CP}} = 0$. (b) $N_{\mathrm{CP}} = N/8$

Fig. 5. Spectral efficiency comparison between LAC-OFDM and its counterparts.

4. Pairwise iterative receiver

4.1. Pairwise iterative receiver design

To fully exploit the antisymmetric characteristics of the AC-OFDM signal and to enhance the BER performance, a pairwise iterative receiver for LAC-OFDM is proposed. In this pairwise receiver, AC-OFDM layers are distinguished from each other and pairwise detection on antisymmetric clipped samples is performed to mitigate the effect of noise (analogous to [23,26] which were developed in the context of ACO-OFDM).

For the l-th AC-OFDM layer, due to the antisymmetry (6) and zero clipping (7), there exists one prior knowledge that one component inside the pair $\left(\tilde{y}_{c,n}^{(l)}, \tilde{y}_{c,n+N_{\mathrm{AC}}(l)}^{(l)}\right)$ $(0 \le n \le N_{\mathrm{AC}}(l) - 1)$ is necessarily zero. As given in [26], the impact on noise can be theoretically cut in half by detecting which sample was clipped at the transmitter and setting it to zero at the receiver. Specifically, after imposing pairwise detection of $\tilde{y}_{c,n}^{(l)}$, an estimate of the l-th layer AC-OFDM signal is given by

$$\left(\tilde{y}_{p,n}^{(l)}, \tilde{y}_{p,n+N_{\mathrm{AC}}(l)}^{(l)}\right) = \begin{cases} (\tilde{y}_{c,n}^{(l)}, 0), & \tilde{y}_{c,n}^{(l)} \ge \tilde{y}_{c,n+N_{\mathrm{AC}}(l)}^{(l)} \\ (0, \tilde{y}_{c,n}^{(l)}), & \tilde{y}_{c,n}^{(l)} < \tilde{y}_{c,n+N_{\mathrm{AC}}(l)}^{(l)} \end{cases}, 0 \le n \le N_{\mathrm{AC}}(l) - 1. \tag{39}$$

Employing pairwise detection following (39), Algorithm 1 presents the pseudocode for this pairwise iterative receiver. Note that a subscript "(i)" is added to all signals to denote the iteration number. As in [23], in the i-th iteration, a more precise estimate of l-th layer AC-OFDM signal is obtained using the pairwise detection (39). Subsequent layers are then updated by removing interference from this layer using this pairwise detected estimate according to (40).

As shown in Sec. 5, as the number of iterations increases the performance of this pairwise receiver converges. In practice, the number of iterations is fixed and denoted I_{m}.

4.2. Computational complexity: pairwise iterative receiver

In each iteration of this pairwise iterative receiver, an additional simple LAC-OFDM receiver step is required in addition to pairwise detection and an additional $N_{\mathrm{AC}}(L)$-point AC-OFDM modulation for the L-th layer. The complexity of pairwise detection is not included in this analysis, since it can be implemented efficiently by logic operations. Hence, the pairwise iterative receiver with I_{m} iterations requires RMOs and RAOs as

Optics EXPRESS

Algorithm 1 Pairwise iterative receiver for LAC-OFDM

Require: Received signals, r_n; Number of layers, L; Constellation set, Ω_X; Maximum number of iterations, I_{m};

Ensure: Detected symbols, $\hat{\mathbf{X}}^{(l),(I_{\mathrm{m}})}$;

1: Calculate $\hat{\mathbf{X}}^{(l),(0)}$ and $\hat{\mathbf{y}}_L^{(l),(0)}$, $l \in [1\ L]$, by using the simple LAC receiver introduced in Sec. II.C (i.e., 0-th iteration)
2: **for** $i = 1 : I_{\mathrm{m}}$ **do**
3: **for** $l = 1 : L$ **do**
4: Create an estimate of layer signal $\widehat{\mathbf{y}'}_L^{(l)}$ by removing previously detected layer signals

$$\widehat{y'}_{L,n}^{(l),(i)} = r_n - \sum_{\nu=1}^{l-1} \alpha_\nu \hat{y}_{L,n}^{(\nu),(i)} - \sum_{\nu=l+1}^{L} \alpha_\nu \hat{y}_{L,n}^{(\nu),(i-1)}. \tag{40}$$

5: Generate $\mathbf{y'}_c^{(l)}$ by averaging according to (16);
6: Calculate $\tilde{\mathbf{y}'}_p^{(l)}$ according to pairwise detector (39);
7: Update $\hat{\mathbf{X}}^{(l),(i)}$ by AC-OFDM demodulation;
8: Update $\hat{\mathbf{y}}_c^{(l),(i)}$ using AC-OFDM modulation;
9: Update $\hat{\mathbf{y}}_L^{(l),(i)}$ by repeating $2^{(l-1)}$ times of $\hat{\mathbf{y}}_c^{(l),(i)}$;
10: **end for**
11: **end for**
12: **return** $\hat{\mathbf{X}}^{(l),(I_{\mathrm{m}})}$;

$$M_{\mathrm{LAC}}^{(\mathrm{PR})}(L,N,I_{\mathrm{m}}) = M_{\mathrm{LAC}}^{(r)}(L,N) + I_{\mathrm{m}}\left(M_{\mathrm{LAC}}^{(r)}(L,N) + M\left(\frac{N}{2^L}\right)\right), \tag{41}$$

$$A_{\mathrm{LAC}}^{(\mathrm{PR})}(L,N,I_{\mathrm{m}}) = A_{\mathrm{LAC}}^{(r)}(L,N) + I_{\mathrm{m}}\left(A_{\mathrm{LAC}}^{(r)}(L,N) + A\left(\frac{N}{2^L}\right)\right). \tag{42}$$

For the improved receiver of LACO-OFDM in [23], pairwise detection is also required. The complexity can be similarly derived as,

$$M_{\mathrm{LA}}^{(\mathrm{IR})}(L,N,I_{\mathrm{m}}) = M_{\mathrm{LA}}^{(r)}(L,N) + I_{\mathrm{m}}\left(M_{\mathrm{LA}}^{(r)}(L,N) + M\left(\frac{N}{2^{L-1}}\right)\right), \tag{43}$$

$$A_{\mathrm{LA}}^{(\mathrm{IR})}(L,N,I_{\mathrm{m}}) = A_{\mathrm{LA}}^{(r)}(L,N) + I_{\mathrm{m}}\left(A_{\mathrm{LA}}^{(r)}(L,N) + A\left(\frac{N}{2^{L-1}}\right)\right). \tag{44}$$

A similar pairwise detector can be applied to the detection of eU-OFDM using the approach in Sec. 4.1 recognizing that half of the samples in the transmitted signal are zero in each layer. In addition, an iterative detector can be implemented using the framework in Algorithm 1 to yield complexity

$$M_{\mathrm{eU}}^{(\mathrm{PR})}(L,N,I_{\mathrm{m}}) = M_{\mathrm{eU}}^{(r)}(L,N) + I_{\mathrm{m}}\left(M_{\mathrm{eU}}^{(r)}(L,N) + \frac{M(N)}{2^L}\right), \tag{45}$$

$$A_{\mathrm{eU}}^{(\mathrm{PR})}(L,N,I_{\mathrm{m}}) = A_{\mathrm{eU}}^{(r)}(L,N) + I_{\mathrm{m}}\left(A_{\mathrm{eU}}^{(r)}(L,N) + \frac{A(N)}{2^L}\right). \tag{46}$$

In contrast to an earlier iterative receiver for eU-OFDM in [27], this approach is likely less complex since it does not require matrix inversion operations in each iteration.

Optics EXPRESS

5. Numerical results

5.1. Computational complexity comparisons

Computational complexity comparisons among the transmitters of LAC- and LACO- and eU-OFDM with different subcarrier number N and layer number L is shown in Fig. 6 and are plotted using the expressions derived in Sec. 3.2. In Fig. 6(a) and (b), the layer number $L = 4$ and in Fig. 6(c) and (d), $N = 1024$. It is evident the transmitter of traditional LACO-OFDM requires the most RMOs as well as RAOs, which is more than twice as the proposed LAC-OFDM. Notice also that the transmitter of eU-OFDM requires slightly more operations than LAC-OFDM.

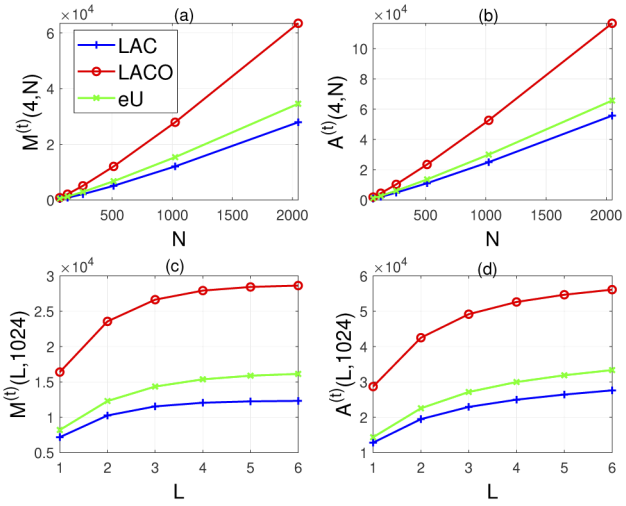

Fig. 6. Transmitter complexity comparison.

Computational complexity comparison among receivers is computed using the expressions in Sec. 3.3 and is shown in Fig. 7. In Fig. 7(a) and (b), L is set to 4, while in Fig. 7(c) and (d), N is set to 1024. As is the case in the transmitter, the relative complexity of LAC-OFDM is the least amongst the techniques considered. Additionally, Fig. 7 demonstrates that the receiver for LACO-OFDM which removes ILI in the time domain is less complex than the receiver for LACO-OFDM removing ILI in the frequency domain. Notice also that the complexity of all receivers is sensitive to N as the dominant term in the complexity analysis arises due to the size of the FFT/IFFT operations. Since LAC-OFDM uses a smaller FFT size, it benefits from reduced complexity. In addition, the complexity saturates with increasing L since the number of degrees of freedom, either in frequency (e.g., LAC- or LACO-OFDM) or in time (e.g., eU-OFDM), in all IM/DD OFDM techniques considered here reduces by half with each increase in layer number. Thus, the incremental increase in complexity must saturate for increasing L.

Consider the case of $N = 1024$ and $L = 4$ for example. Table 1 provides a summary of the number of real addition and multiplication operations required for each IM/DD OFDM approach. Clearly, LACO-OFDM requires the most operations while LAC-OFDM requires the smallest number. Notice that the transmitter for LACO-OFDM requires more than twice the number of RMOs as LAC-OFDM while for the receiver LAC-OFDM requires nearly one-third of the number of RMOs as LACO-ODFM with receiver designed in [11] according to (27).

Computational complexity comparison among the pairwise iterative receivers for different number of iterations are computed according to the expressions in Sec. 4.2 and is shown in Fig. 8, where $L = 4$ and $N = 1024$. The complexity of the simple receivers is denoted with $I_m = 0$ iterations. For all the pairwise iterative receivers, the computational complexity increases linearly

Optics EXPRESS

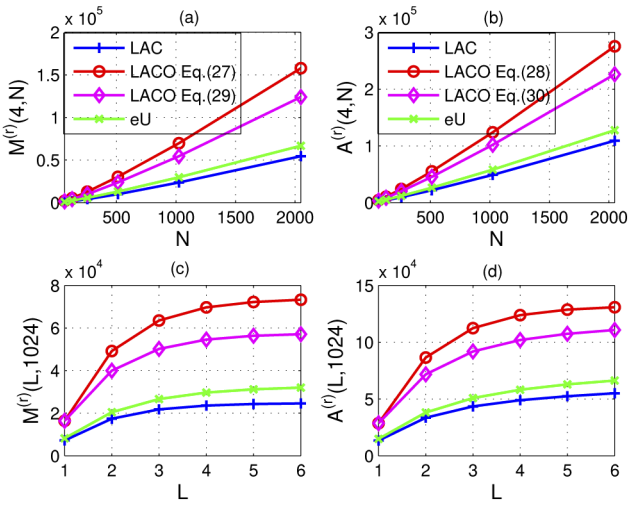

Fig. 7. Receiver complexity comparison.

Table 1. Complexity comparison of LAC-, LACO- and eU-OFDM (N = 1024 and L = 4)

	$M^{(t)}$	$A^{(t)}$	$M^{(r)}$	$A^{(r)}$
LAC	12048	24968	23580	48974
LACO	27920	52616	69660	123790
eU	15364	29954	29703	58180

with I_m. For a given I_m, the pairwise iterative receiver for LAC-OFDM is the least complex among the three schemes. Additionally, as I_m increases, the gap between number of RMOs (or RAOs) for the pairwise receiver for LAC-OFDM and that for LACO-OFDM increases. This also holds for the gap between the pairwise iterative receivers for LAC- and eU-OFDM.

5.2. BER performance

Define the optical signal-to-noise ratio (OSNR) as OSNR $= 10\log_{10}(P_{\mathrm{o}}/\sigma_w)$ (dB) where P_{o} is total average optical power [28]. A flat channel with AWGN is assumed in the simulation [8,9] and QAM constellations normalized to unit average energy with Gray labelling are utilized.

Like LACO-OFDM, each layer AC-OFDM signal follows a clipped Gaussian distribution and the total average optical power is given by [18]

$$P_{\mathrm{o}} = \sum_{l=1}^{L} \frac{\alpha_l \sigma_l}{\sqrt{2\pi}} \tag{47}$$

where $\sigma_l = \sqrt{\mathrm{E}\{|x_n^{(l)}|^2\}}$ is the standard deviation of $x_n^{(l)}$.

For the l-th layer AC-OFDM, $\mathbf{y}_c^{(l)}$ is repeated 2^{l-1} times based on (14) similar to LACO-OFDM in [11]. Thanks to this inherent repetition code, the electrical SNR at k-th subcarrier assuming the clipping distortion removed completely is given by

$$\mathrm{SNR}_k^{(l)} = 2^{l-1}\alpha_l^2 \frac{\mathrm{E}\{|X_k^{(l)}|^2\}}{2\sigma_w^2} \overset{(a)}{=} 2^{l-1}\alpha_l^2 \frac{\mathrm{E}\{|x_n^{(l)}|^2\}}{2\sigma_w^2} = \frac{2^{l-2}\alpha_l^2\sigma_l^2}{\sigma_w^2} \tag{48}$$

Optics EXPRESS

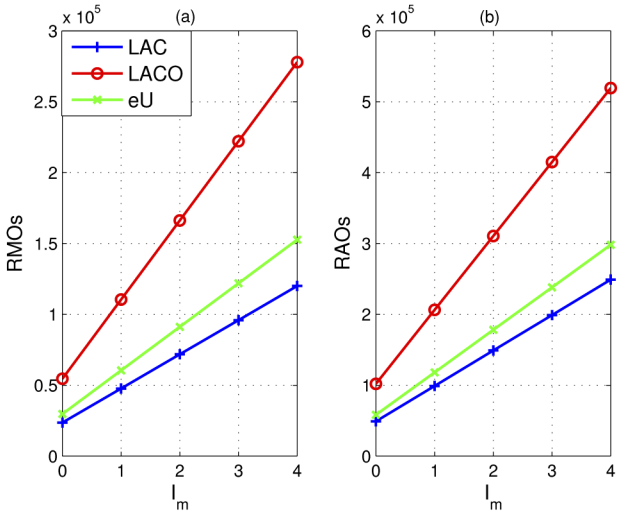

Fig. 8. Computational complexity comparison among the pairwise iterative receivers for LAC- and LACO- and eU-OFDM for different number of iterations ($L = 4$ and $N = 1024$ are used).

where (a) is due to Parseval's theorem [25]. When the power allocation factor is set as [9,11,18]

$$\alpha_1 : \alpha_2 : \cdots : \alpha_L = 1 : 2^{-\frac{1}{2}} : \cdots : 2^{-\frac{L-1}{2}}, \text{and } \alpha_1 = 1, \tag{49}$$

then

$$\mathrm{SNR}_k^{(l)} = \frac{\mathrm{E}\{\|X_k^{(l)}\|^2\}}{2\sigma_w^2}, \ 1 \le l \le L. \tag{50}$$

If the same constellation is used in all layers, the SNR of all data-bearing subcarriers in all layers will be the same. Using the formula for BER of QAM [24], a bound on the BER of AC-OFDM is given by

$$\mathrm{BER}_{\mathrm{AC}}^{(l)} \approx \frac{4(\sqrt{M_l}-1)}{\sqrt{M_l}\log_2 M_l} Q\left(\sqrt{\frac{3}{M_l-1}\mathrm{SNR}_k^{(l)}}\right). \tag{51}$$

Then a bound on the BER of LAC-OFDM is given by

$$\mathrm{BER}_{\mathrm{LAC}} = \frac{\sum_{l=1}^{L} \mathrm{BER}_{\mathrm{AC}}^{(l)} 2^{-l}\log_2 M_l}{\sum_{l=1}^{L} 2^{-l}\log_2 M_l}. \tag{52}$$

Since pairwise detection can at best cut the impact of noise in half at the receiver side [23,26], $\mathrm{SNR}_k^{(l)}$ in (49) can be enhanced by at most 3-dB by using the pairwise iterative receiver. Hence, a theoretical BER approximation for the proposed pairwise iterative receiver can be obtained as

$$\mathrm{BER}_{\mathrm{LAC,\,PR}} = \frac{\sum_{l=1}^{L} \mathrm{BER}_{\mathrm{AC,\,PR}}^{(l)} 2^{-l}\log_2 M_l}{\sum_{l=1}^{L} 2^{-l}\log_2 M_l} \tag{53}$$

where

$$\mathrm{BER}_{\mathrm{AC,\,PR}}^{(l)} \approx \frac{4(\sqrt{M_l}-1)}{\sqrt{M_l}\log_2 M_l} Q\left(\sqrt{\frac{6}{M_l-1}\mathrm{SNR}_k^{(l)}}\right). \tag{54}$$

The BER performance comparison among LAC-, LACO- and eU-OFDM is shown for each layer in Fig. 9(a) where $N = 1024$, $L = 4$ and 16-QAM are utilized. It can be seen that all

Optics EXPRESS

schemes have nearly the same performance. As discussed in Sec. 3.4, the spectral efficiency of these three techniques are also nearly identical. Thus, LAC-OFDM provides the same BER performance as LACO- and eU-OFDM while remaining less complex. In addition, the theoretical BER bound of LAC-OFDM according to (52) is presented, which indicates the theoretical BER is aligned well with simulated results especially in the high OSNR regime.

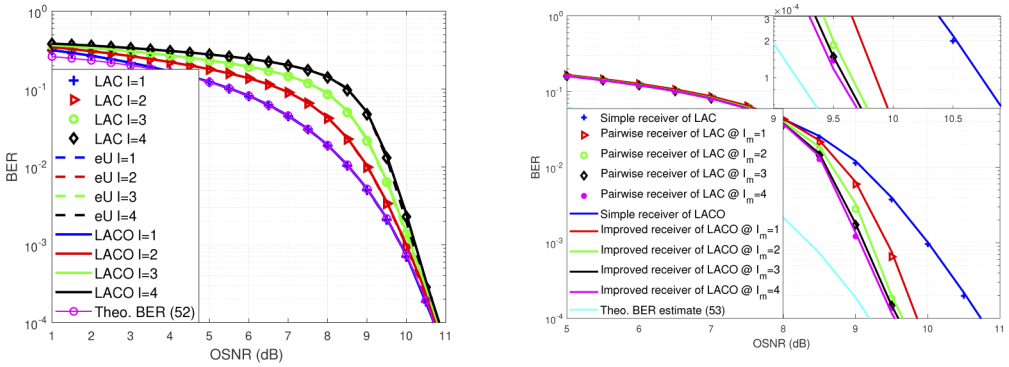

(a) BER of each layer.

(b) BER of the pairwise iterative receiver

Fig. 9. BER performance comparison between LAC-OFDM and its counterparts ($N = 1024$ and $L = 4$). Note 'Theo.' denotes the 'theoretical'.

The BER performance of the proposed pairwise iterative receiver of LAC-OFDM for different number of iterations is shown in Fig. 9(b), in which the performance of improved receiver of LACO-OFDM in [23] is also presented. In all cases, $N = 1024$, $L = 4$ and 16-QAM are utilized. The pairwise iterative receiver of LAC-OFDM achieves nearly the same performance as the improved receiver for LACO-OFDM in [23] while remaining less complex as shown in Fig. 8. At BER $= 10^{-4}$, for $I_m = 1,\ 2,\ 3$ and 4, the pairwise iterative receiver achieves about 0.88 dB, 1.08 dB, 1.15 dB and 1.19 dB OSNR gains compared to the simple receiver, respectively. Although the BER performance becomes better as I_m increases from 1 to 4, the relative improvement decreases with I_m. Additionally, the theoretical BER estimate according to (53) is presented, which is aligned well with simulated results in the high OSNR regime.

Consider the complexity constrained design examples in Table 2 where the two cases have nearly same computational complexity. In Case 1, the pairwise iterative receiver of LAC-OFDM employs one iteration while LACO-OFDM employs no iterations. Though the receivers in this scenario require approximately the same complexity, LAC-OFDM achieves a 0.88 dB OSNR gain over LACO-OFDM at BER $= 10^{-4}$. In Case 2, the pairwise iterative receiver for LAC-OFDM employs 3 iterations while LACO-OFDM employs a single iteration. In Case 2, the both schemes have nearly the same complexity, however, the pairwise iterative receiver for LAC-OFDM achieves 0.27 dB gain over the improved LACO-OFDM receiver [23] at BER $= 10^{-4}$.

Table 2. Comparison between pairwise receivers for LAC- and LACO-OFDM with nearly same complexity and their gain compared to corresponding simple ($I_m = 0$) receivers at BER $= 10^{-4}$ ($N = 1024$ and $L = 4$)

		RMOs	RAOs	Gain
Case 1	LAC @ $I_m = 1$	47676	98974	0.88 dB
	LACO @ $I_m = 0$	54556	101902	0 dB
Case 2	LAC @ $I_m = 3$	95868	198974	1.15 dB
	LACO @ $I_m = 1$	110396	206238	0.88 dB

Optics EXPRESS

5.3. PAPR performance

The PAPR of the transmitted signal $\mathbf{z}$ is defined as [29]

$$\text{PAPR} = \frac{\max\limits_{0\le n\le N-1} z_n^2}{\text{E}\{z_n^2\}}. \tag{55}$$

The complementary cumulative distribution function (CCDF) of the PAPR is defined as [30] $\text{CCDF}(\xi) = \Pr\{\text{PAPR}>\xi\}$ where $\Pr\{\Pi\}$ denotes the probability of an event Π.

Figure 10 compares the CCDF of the PAPR for a variety of LAC-OFDM with related schemes where $N = 1024$. The power allocation factor is set according to (49). Notice that the PAPR performance of LAC-OFDM closely mirrors that of LACO-OFDM with the same number of layers. This is because each layer of LAC-OFDM follows the same clipped Gaussian distribution as the ACO-OFDM layers in LACO-OFDM. The total signal distribution of LAC-OFDM is thus the same as LACO-OFDM for a given number of layers. The PAPR of eU-OFDM is higher than LAC- and LACO-OFDM for the same number of layers. Therefore, LAC-OFDM has the same PAPR as LACO-OFDM while remaining less complex to implement.

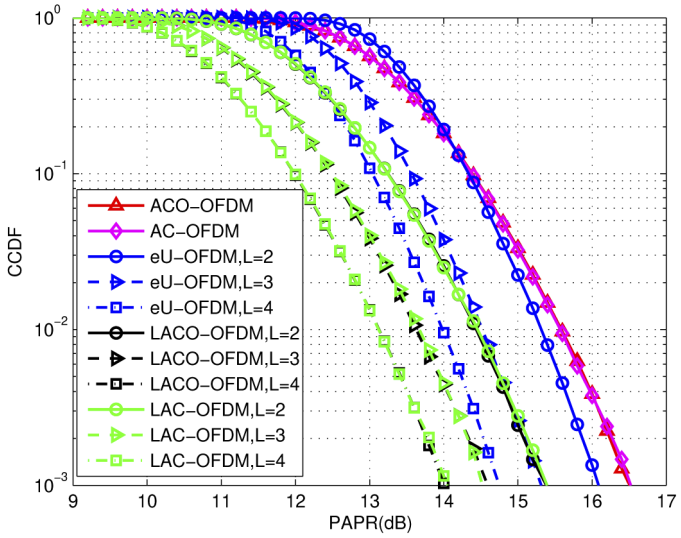

Fig. 10. PAPR comparison between LAC-OFDM and its counterparts with $N = 1024$ subcarriers.

6. Conclusions

In this paper, a new approach for the construction of IM/DD OFDM signalling is given. Low-complexity AC-OFDM is proposed where antisymmetry is imposed in time-domain to make satisfying the non-negatively constraint straightforward. To improve spectral efficiency, LAC-OFDM is then proposed, which consists of L superimposed layers of AC-OFDM much like traditional LACO- and eU-OFDM. Exploiting the special structure of the antisymmetry, a pairwise iterative receiver is also proposed for LAC-OFDM, which can significantly enhance the BER performance.

Our analysis shows that for the same number of layers/streams LAC-OFDM is less complex than existing LACO- and eU-OFDM methods both for the transmitter and receiver while preserving the same BER performance. LAC-OFDM has the same PAPR performance as LACO-OFDM and a smaller PAPR than eU-OFDM. Additionally, at the same complexity, LAC-OFDM can

Optics EXPRESS

perform more iterations than LACO-OFDM resulting in a gain in power efficiency. In particular, the pairwise iterative receiver for LAC-OFDM with one iteration requires nearly the same computational complexity as the simple receiver of LACO-OFDM while providing a 0.88 dB OSNR gain at BER = 10^{-4}. The development of low complexity optical OFDM signalling is especially important in VLC systems due to the requirement to maintain energy efficient illumination from the luminaire.

In this paper, the emphasis is on presenting the central concept of AC- and LAC-OFDM and on transceiver design and complexity analysis for LAC-OFDM for low-complexity VLC systems. Future work includes quantifying the performance on dispersive channels as well as experimental verification.

Funding. Natural Sciences and Engineering Research Council of Canada.

Acknowledgment. The authors would like to thank Prof. Zhaocheng Wang for helpful discussions and for providing sample code on iterative receiver for LACO-OFDM to aid in comparison with [23].

Disclosures. The authors declare no conflicts of interest.

References

1. L. Hanzo, H. Haas, S. Imre, D. O'Brien, M. Rupp, and L. Gyongyosi, "Wireless myths, realities, and futures: from 3G/4G to optical and quantum wireless," Proc. IEEE **100**(Special Centennial Issue), 1853–1888 (2012).
2. J. M. Kahn and J. R. Barry, "Wireless infrared communications," Proc. IEEE **85**(2), 265–298 (1997).
3. H. Haas, J. Elmirghani, and I. White, "Optical wireless communication," Phil. Trans. R. Soc. A **378**(2169), 20200051 (2020).
4. M. Z. Chowdhury, M. K. Hasan, M. Shahjalal, M. T. Hossan, and Y. M. Jang, "Optical wireless hybrid networks: Trends, opportunities, challenges, and research directions," IEEE Commun. Surv. Tutorials **22**(2), 930–966 (2020).
5. R. Bai, Q. Wang, and Z. Wang, "Asymmetrically clipped absolute value optical OFDM for intensity-modulated direct-detection systems," J. Lightwave Technol. **35**(17), 3680–3691 (2017).
6. H. G. Olanrewaju, J. Thompson, and W. O. Popoola, "Pairwise coding for mimo-ofdm visible light communication," IEEE Trans. Wireless Commun. **19**(2), 1210–1220 (2020).
7. J. Armstrong, "OFDM for optical communications," J. Lightwave Technol. **27**(3), 189–204 (2009).
8. S. D. Dissanayake and J. Armstrong, "Comparison of ACO-OFDM, DCO-OFDM and ADO-OFDM in IM/DD systems," J. Lightwave Technol. **31**(7), 1063–1072 (2013).
9. D. Tsonev and H. Haas, "Avoiding spectral efficiency loss in unipolar OFDM for optical wireless communication," in *2014 IEEE International Conference on Communications (ICC)*, (2014), pp. 3336–3341.
10. N. Fernando, Y. Hong, and E. Viterbo, "Flip-ofdm for unipolar communication systems," IEEE Trans. Commun. **60**(12), 3726–3733 (2012).
11. Q. Wang, C. Qian, X. Guo, Z. Wang, D. G. Cunningham, and I. H. White, "Layered ACO-OFDM for intensity-modulated direct-detection optical wireless transmission," Opt. Express **23**(9), 12382–12393 (2015).
12. M. S. Islim, D. Tsonev, and H. Haas, "On the superposition modulation for OFDM-based optical wireless communication," in *2015 IEEE global conference on signal and information processing (GlobalSIP)*, (IEEE, 2015), pp. 1022–1026.
13. H. Elgala and T. D. Little, "SEE-OFDM: Spectral and energy efficient OFDM for optical IM/DD systems," in *2014 IEEE 25th annual international symposium on personal, indoor, and mobile radio communication (PIMRC)*, (IEEE, 2014), pp. 851–855.
14. Q. Wang, B. Song, B. Corcoran, D. Boland, C. Zhu, L. Zhuang, and A. J. Lowery, "Hardware-efficient signal generation of layered/enhanced ACO-OFDM for short-haul fiber-optic links," Opt. Express **25**(12), 13359–13371 (2017).
15. J. Zhou and W. Zhang, "A comparative study of unipolar OFDM schemes in Gaussian optical intensity channel," IEEE Trans. Commun. **66**(4), 1549–1564 (2018).
16. S. Mazahir, A. Chaaban, H. Elgala, and M.-S. Alouini, "Achievable rates of multi-carrier modulation schemes for bandlimited IM/DD systems," IEEE Trans. Wireless Commun. **18**(3), 1957–1973 (2019).
17. X. Zhang, S. Chen, and L. Hanzo, "On the discrete-input continuous-output memoryless channel capacity of layered ACO-OFDM," J. Lightwave Technol. **38**(18), 4955–4968 (2020).
18. R. Bai and S. Hranilovic, "Absolute value layered ACO-OFDM for intensity-modulated optical wireless channels," IEEE Trans. Commun. **68**(11), 7098–7110 (2020).
19. A. J. Lowery, "Spectrally efficient optical orthogonal frequency division multiplexing," Phil. Trans. R. Soc. A **378**(2169), 20190180 (2020).
20. X. Liu, J. Li, J. Li, and Z. Huang, "Analysis of the single-FFT receiver for layered ACO-OFDM in visible light communications," J. Lightwave Technol. **38**(17), 4757–4764 (2020).
21. R. Bai and S. Hranilovic, "Layered antisymmetry-constructed clipped optical OFDM for IM/DD systems," in *2019 IEEE Global Communications Conference (GLOBECOM)*, (IEEE, 2019), pp. 1–6.

Optics EXPRESS

22. T. Zhang, L. Sun, C. Zhao, S. Qiao, and Z. Ghassemlooy, "Low-complexity receiver for HACO-OFDM in optical wireless communications," IEEE Wireless Commun. Lett. **10**(3), 572–575 (2021).
23. Q. Wang, Z. Wang, X. Guo, and L. Dai, "Improved receiver design for layered ACO-OFDM in optical wireless communications," IEEE Photonics Technol. Lett. **28**(3), 319–322 (2016).
24. D. Tsonev, S. Videv, and H. Haas, "Unlocking spectral efficiency in intensity modulation and direct detection systems," IEEE J. Select. Areas Commun. **33**(9), 1758–1770 (2015).
25. B. Porat, A course in digital signal processing (Wiley, 1997).
26. K. Asadzadeh, A. Dabbo, and S. Hranilovic, "Receiver design for asymmetrically clipped optical OFDM," in *2011 IEEE GLOBECOM Workshops (GC Wkshps)*, (IEEE, 2011), pp. 777–781.
27. J. Dang, Z. Zhang, and L. Wu, "Improving the power efficiency of enhanced unipolar OFDM for optical wireless communication," Electron. Lett. **51**(21), 1681–1683 (2015).
28. M. S. Mossaad, S. Hranilovic, and L. Lampe, "Visible light communications using OFDM and multiple LEDs," IEEE Trans. Commun. **63**(11), 4304–4313 (2015).
29. J. Wang, Y. Xu, X. Ling, R. Zhang, Z. Ding, and C. Zhao, "PAPR analysis for OFDM visible light communication," Opt. Express **24**(24), 27457–27474 (2016).
30. M. Gao, C. Li, and Z. Xu, "Optimal transmission of VLC system in the presence of LED nonlinearity and APD module saturation," IEEE Photonics J. **10**(5), 1–14 (2018).